JOURNAL OF MATERIALS SCIENCE 27 (1992) 101–106

Ostwald ripening of silver in glass

K. YATA, T. YAMAGUCHI
Faculty of Science and Technology, Keio University, 3-14-1 Hiyoshi Kohokuku, Yokahama, 223 Japan

The Ostwald ripening theory developed in metals and ceramics was applied to a silver–glass system. Experimental results showed that growth kinetics of silver particles obey the Ostwald ripening mechanism. The particle size distribution, however, was inconsistent with the theory, probably because of other factors not included in the Ostwald ripening theory. Modified equations failed to explain the experimental results. Values for the interfacial energy were obtained using the modified theory and sessile drop method.

1. Introduction

Silver–glass thick film conductors have been used extensively in electronic applications. The microstructure of thick films influences their electrical properties. The process and mechanism of thick film formation has hardly been investigated [1, 2]. Recent investigations showed that the formation process of thick films was influenced by the glass which acts as a liquid phase during firing [3]. The forming process should, therefore, be regarded as liquid phase sintering of silver. Information on the silver–glass interaction which is required to evaluate the liquid phase sintering of silver, however, is not available. As a first step to apply the theory of liquid phase sintering [4–7] to the silver–glass system, the growth of silver particles in glass was studied and the experimental results were analysed using the Ostwald ripening theory.

Silver particles dispersed in glass were annealed isothermally and their growth was observed with a scanning electron microscope (SEM). The growth of particles was determined with an image-analyser numerically and the results were compared with the Ostwald ripening theory. The kinetics of growth agreed with the theory, but particle size distributions did not. The value of interfacial energy calculated by the modified theory was compared with that estimated by the sessile drop method.

2. Theory

Ostwald ripening was first discussed by Greenwood [8] theoretically. In his argument, the concentration c_p of solute at the particle–matrix interface in equilibrium with a particle of radius r was given by the Gibbs–Thomson equation

$$c_p = c_e \exp\left(\frac{2\gamma V_m}{RT}\right) \quad (1)$$

where c_e is the solute concentration in equilibrium with a particle of infinite size, γ the interfacial energy between solute and solvent, V_m the molar volume of solute, R the gas constant and T the temperature. The diffusion of the solute was given by Fick's law,

$$j = D\left(\frac{\partial c}{\partial r}\right) \quad (2)$$

where j is the diffusion flux, D the diffusion coefficient and c the concentration.

Ostwald ripening was discussed more exactly and the LSW theory was developed by Lifshits and Slyozov [9] and Wagner [10]. According to the LSW theory, diffusion and reaction at the interface are rate determining processes. In most alloy systems, growth of particles is diffusion controlled, which will be discussed below.

Two equations are derived from the LSW theory.

(a) Relation between annealing time and mean radius is given by

$$\bar{r}^3 - \bar{r}_0^3 = Kt \quad (3)$$

where $\bar{r}$ is the mean radius at time t and $\bar{r}_0$ the initial mean radius. The proportionality constant K is given by

$$K = \frac{8\gamma D V_m^2 c_e}{9RT} \quad (4)$$

(b) The particle size distribution is steady state distribution independent of annealing time. Assuming $\rho = r/\bar{r}$, the steady state distribution $f(\rho)$ is given by

$$f(\rho) = \rho^2 h(\rho) \quad (5)$$

where the function $h(\rho)$ was given by

$$h(\rho) = \begin{cases} \left(\frac{3}{3+\rho}\right)^{\frac{7}{3}} \left(\frac{1.5}{1.5-\rho}\right)^{\frac{11}{3}} \exp\left(\frac{-\rho}{1.5-\rho}\right) & \rho < 3/2 \\ 0; & \rho \geqslant 3/2 \end{cases} \quad (6)$$

The growth of particles was observed and compared with the LSW theory in alloy systems [11–16]. The comparison showed that the relation between annealing time and mean radius obeyed the theory, but that the particle size distribution did not. This is

0022–2461/92 $03.00 + .12

probably because of neglecting other factors that influence Ostwald ripening. Jayanth and Nash [17] discussed these factors.

The effect of volume fraction of particles has been reported by many authors [18–26]. Modified kinetics and particle size distribution equations were proposed, assuming the interaction between diffusion fields. According to the modified equations, an increase in volume fraction promotes growth of particles and broadens the particle size distribution. The modified equations fail, however, to explain Ostwald ripening perfectly.

Other factors were studied. At first, coalescence of particles [21, 27] changes the diffusion fields because coalescence is caused by the overlap of diffusion fields or by the attraction to eliminate lattice mismatch between matrix and particles at close interparticle distances. Next, accumulation of elastic stress by growth [28–30] changes the rate determining process and causes mass transfer from large particles to small particles. Furthermore, it was shown that short-circuit diffusion [31], the motion of particles [32, 33] and thermodynamic non-ideality [34–36] also influence Ostwald ripening. The modified theories still fail to explain the Ostwald ripening phenomenon exactly because each modified theory usually contains only one factor. It is thus meaningful to incorporate several factors into the LSW theory to fully explain the Ostwald ripening phenomenon.

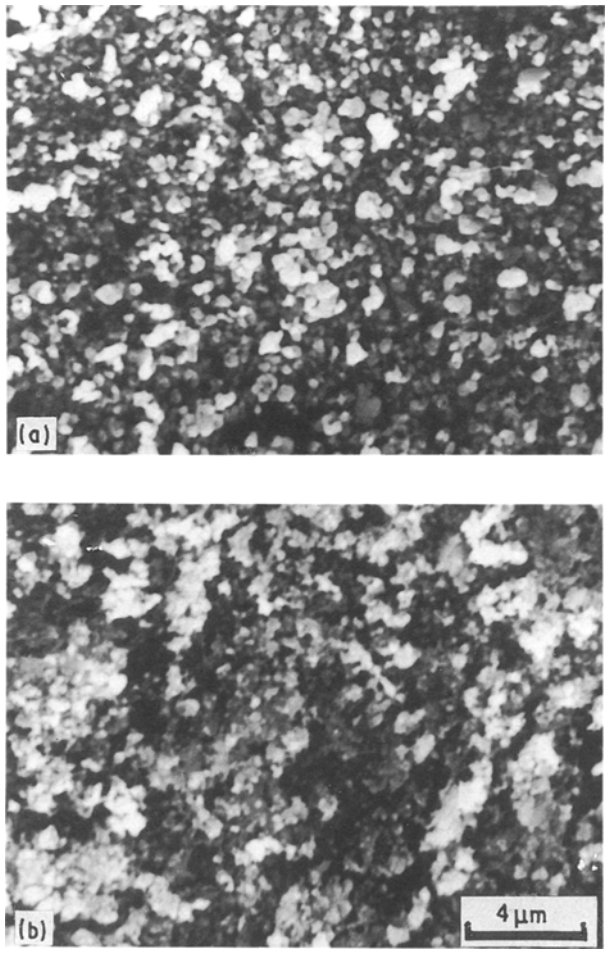

Figure 1 SEM photos of silver powders; (a) coarse and (b) fine.

3. Experimental procedure

3.1. Materials

Two kinds of commercial silver powders, coarse and fine, were used. The coarse powder is spherical K-ED (M. M. Corporation) with a mean radius of 0.2 μm, and the fine powder is spherical K-12 (SMM Corporation) with a mean radius of 0.04 μm. Fig. 1 shows SEM photos of these powders.

Table I shows the composition of the glass. This glass did not decompose or crystallize throughout the annealing process studied. The glass was prepared as follows. Starting oxides were mixed and melted in a platinum crucible at 1300 °C, and the melt was quenched. The obtained glass was milled with a ball mill using ethanol. The density of the glass is 3.7 g cm^{-3} and the softening point is 608 °C.

3.2. Particle growth of silver in glass

Before studying the growth of particles, specimens with several mixing ratios of glass and silver powder were prepared to determine the optimum mixing ratio. Powder mixtures of silver and glass containing 10 to 20 wt % silver were heated in a quartz crucible at 600 °C for 1 h and quenched into water. Their cross-sections were observed with an SEM. Many particles coalesced at 20 wt % silver, and a small number of particles were observed at 10 wt % silver. In addition, specimens containing many fine particles were not suitable for SEM observation because of the limit of resolution. The mixture of 10 wt % coarse powder and 5 wt % fine powder was chosen as the optimum mixing ratio.

TABLE I Glass composition in wt%

PbO	SiO_2	B_2O_3	Al_2O_3
55.00	30.00	9.90	5.10

The silver powders and glass frit were mixed in the determined ratio, heated in a quartz crucible at 800 °C for 1 h and cooled slowly to eliminate pores in glass and to saturate the glass with silver. Next, the specimens were annealed in a furnace held at 600 °C for 1 to 168 h and quenched into water. The quenched specimens were polished and etched in 0.5 N nitric acid. Four photos were taken of each specimen and were modified manually for effective image analysis. The modified photos were analysed with an image analyser and particle size distributions of silver were obtained. Particle size distributions in three dimensions were determined according to stereology (Schwartz–Saltykov method [37]) assuming that particles are spherical.

4. Results and discussion

4.1. Growth of silver particles in glass

Fig. 2 shows SEM photos and particle size distributions. For annealing times of less than 4 h, the particle size decreased because silver dissolved into the glass to

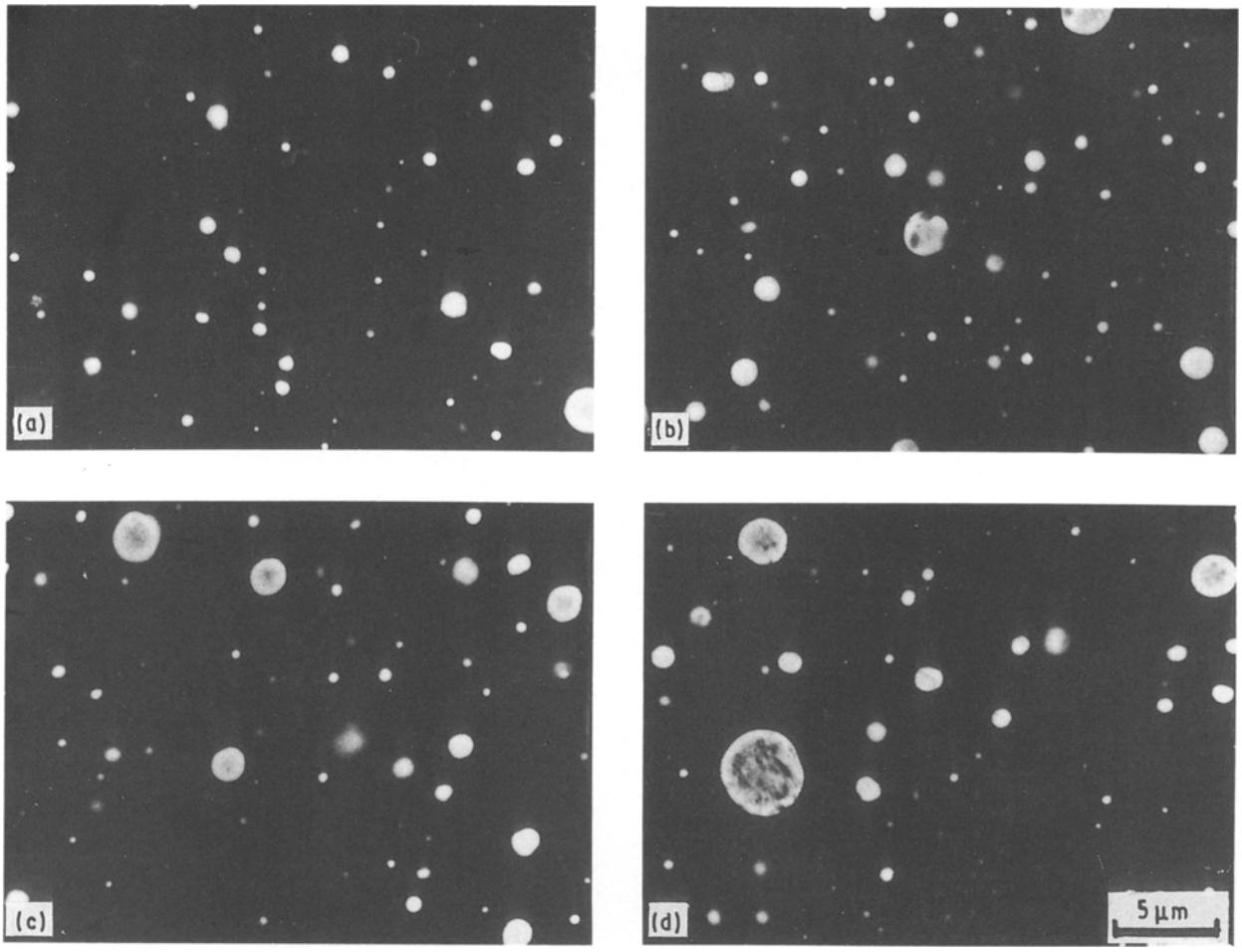

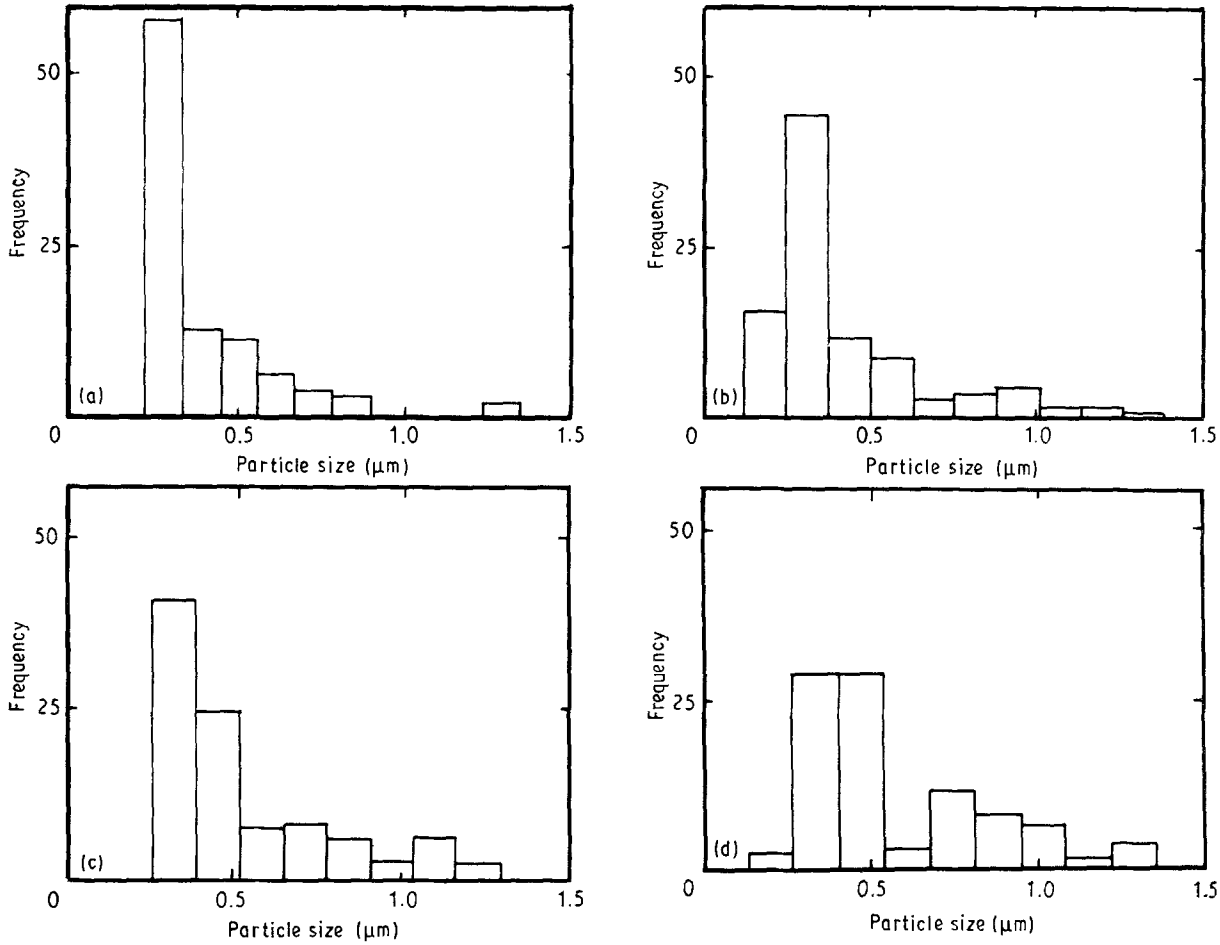

Figure 2 Cross-section of specimens and the particle size distributions of silver calculated by stereology. Annealed for (a) 4 h, (b) 51 h, (c) 125 h and (d) 168 h.

achieve an equilibrium concentration. After the equilibrium was established, growth of silver particles occurred. The growth process after 4 h was, therefore, studied.

The frequency of particles below 0.2 μm in diameter is much lower than that expected by the LSW theory, for which two possible factors are responsible. Firstly, small particles below 0.2 μm were not detectable by SEM and with the image-analyser. Particles below 1 mm in diameter on photos, equivalent to below 0.2 μm in diameter on specimens, were neglected in the calculation of stereology because they were not separable from signal noise. Secondly, the Schwartz–Saltykov method tends to emphasize the larger particles.

4.2. Kinetics of growth

Equation 3 was tested with our experimental data. Fig. 3 shows that the cube of the mean radius is proportional to the annealing time, i.e. it suggests that silver particles grew by the Ostwald ripening mechanism. The proportionality constant for the kinetic equation of the LSW theory, K, was 5×10^{-26} m^3 s^{-1}.

The volume fraction of silver was calculated to be 5.9%, assuming that all the silver in the glass precipitates on annealing. Fig. 4 shows the effect of the volume fraction on K for some models. The broken line in Fig. 4 is for the volume fraction of 5.9%. Values of K scattered depending on the model and each model failed to explain the Ostwald ripening of silver particles. Factors other than volume fraction are probably responsible for such behaviour.

4.3. Particle size distribution

At first, some normalized particle size distributions according to Ardell [12] were compared with theoretical equations by the LSW theory and then with the modified one by the BW model in Fig. 5, in which the full line is the distribution curve predicted by the LSW theory and the broken line, by the BW model. Observed particle size distributions do not agree with the theoretical ones. This result suggests that the particle size distribution is dependent on other factors not included in Equation 3, which will be discussed below.

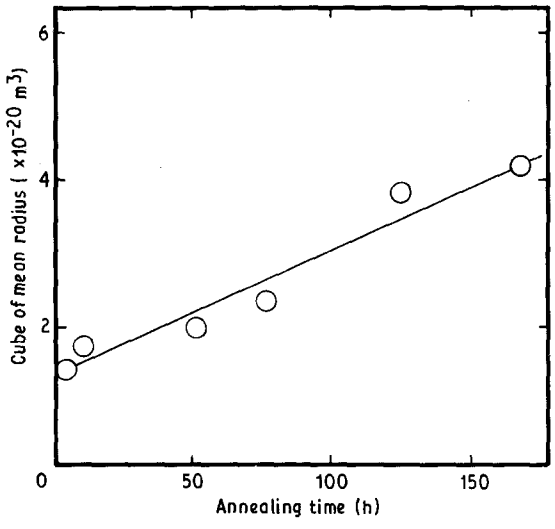

Figure 3 Plot of cube of mean radius against annealing time.

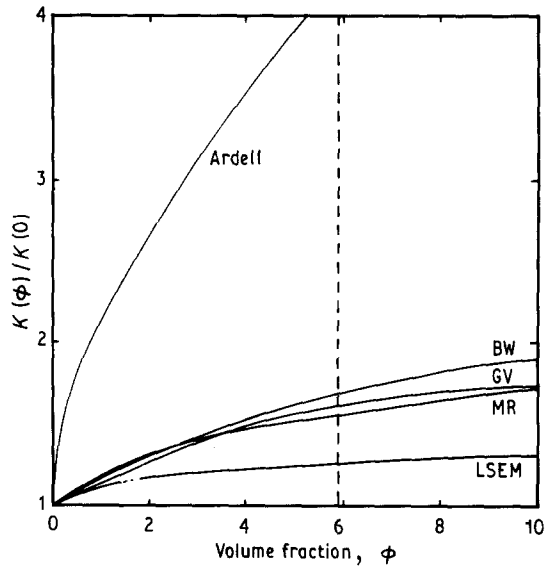

Figure 4 Variation of K with volume fraction according to models. The broken line is for the volume fraction of 5.9%.

Firstly, coalescence of silver particles is negligible, because of a small volume fraction of silver particles. Secondly, elastic stress by growth is relaxed by the softening of the glass matrix. The effect of short-circuit diffusion cannot be evaluated because of no available data. Next, the motion of particles by gravity should not be responsible because the sedimentation distances of 0.1 and 1 μm particles are 10^{-6} and 10^{-4} μm in 168 h, respectively, as calculated by the Stokes equation. Finally, non-ideality of solution is negligible because of the small volume fraction of silver particles and a small solubility of silver in glass.

The above discussion implies that it is impossible to explain the difference in particle size distributions between experimental results and theories. Other factors may also be responsible for Ostwald ripening of silver particles.

4.4. Estimation of interfacial energy

Estimation of the interfacial energy between silver and glass was attempted using a modified theory. The values of K at 5.9 vol % of silver which was calculated by different models (BW, GV and MR model) were almost the same, hence the K value by GV model was used for estimation. Details of estimation are given in the Appendix. The calculated interfacial energy is 0.4 J m^{-2} for the diffusion of ions and 0.1 J m^{-2} for the diffusion of atoms. The interfacial energy estimated by the sessile drop method [38] was 1.0 J m^{-2}. These results suggest that it is plausible that silver ions, not atoms, diffuse in glass. Terai *et al.* [39] discussed the ionic diffusion of silver in glass containing alkali metal oxides and Kaneko [40] showed that an electric field promotes the diffusion of silver in glass.

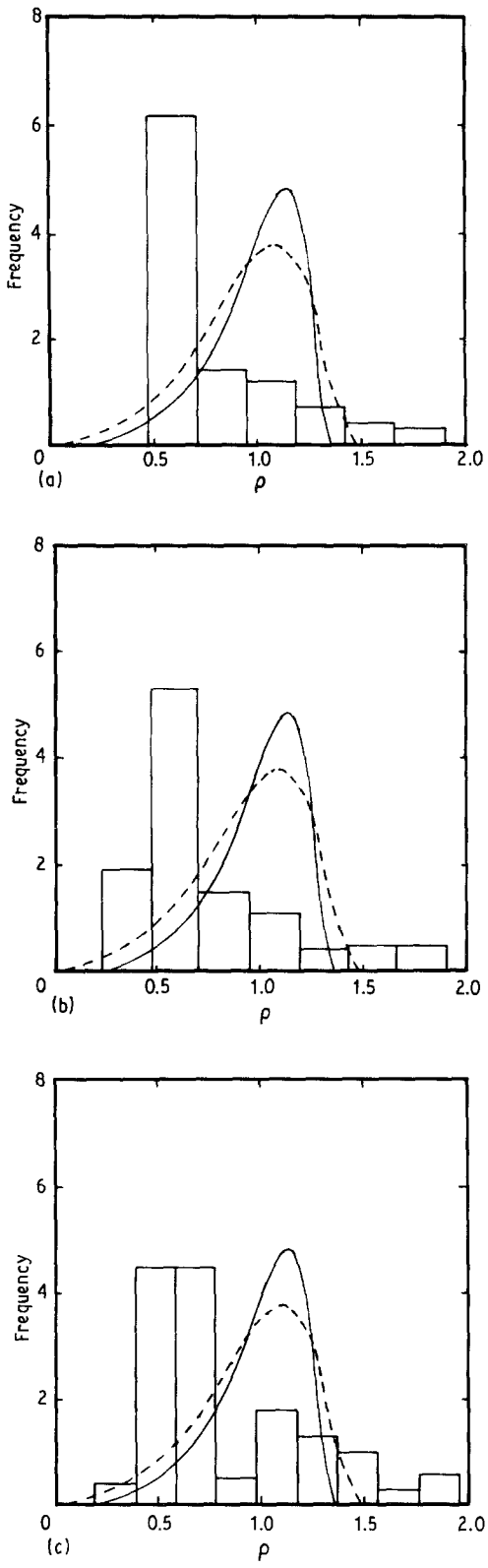

Figure 5 Normalized particle size distributions according to Ardell [12]. The full line is the theoretical distribution curve by the LSW theory and the broken line, BW model. Annealed for (a) 4 h, (b) 51 h and (c) 168 h.

5. Conclusion

Silver particles grew in glass by the Ostwald ripening mechanism. The particle size distribution was not successfully explained by previously reported theories. The theory in which some factors such as volume fraction are taken into account could describe the Ostwald ripening of silver particles semiquantitatively.

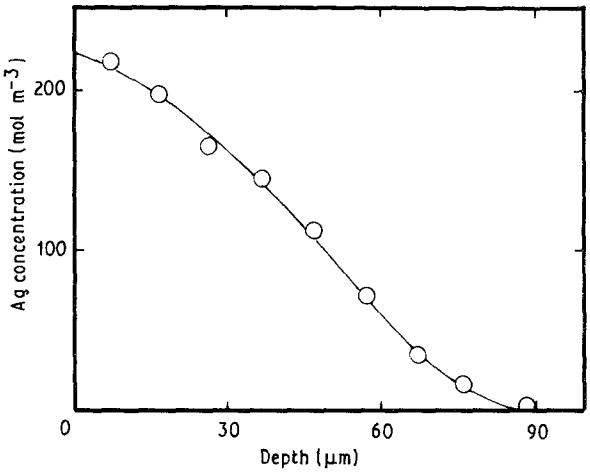

Figure 6 Concentration profile of silver in the glass.

Appendix

According to the GV model, K is given by

$$K = \frac{8\gamma D V_m^2 c_e \alpha^3}{9RT(1 - \phi^{1/3})} \quad \text{(A1)}$$

where α is the constant dependent on the volume fraction ϕ. In Equation A1 D, c_e and γ are unknown. D and c_e were measured by the diffusion couple method. The experimental procedure is as follows. The surface of glass was coated with silver, annealed at 600 °C for 3 h and quenched into water. The cross-section normal to the coated surface was polished. Silver was analysed with an electron probe micro-analyser (EPMA) using the ZAF method (for oxides). Fig. 6 shows the concentration profile of silver in glass. The diffusion coefficient was calculated as $2.1 \times 10^{-13}\,m^2\,s^{-1}$ by Fick's law. The solubility of silver was given by the concentration at the interface, $217\,mol\,m^{-3}$. From Equation A1, the interfacial energy is given by

$$\gamma = \frac{9KRT(1 - \phi^{1/3})}{8DV_m^2 c_e \alpha^3} \quad \text{(A2)}$$

where V_m is $3.73 \times 10^{-6}\,m^3\,mol^{-1}$ diffusing as ions or $7.52 \times 10^{-6}\,m^3\,mol^{-1}$ diffusing as atoms. Substituting these values into Equation A2, the interfacial energy was calculated to be $0.1\,J\,m^{-2}$ for the diffusion of atoms or $0.4\,J\,m^{-2}$ for ions.

The calculated interfacial energies were compared with the value estimated from the experimental data by the sessile drop method (Adams's Table [38]). According to the method, the interfacial energy was calculated as $1.0\,J\,m^{-2}$ at 600 °C.

Acknowledgement

The authors gratefully thank TDK Corporation for assistance with this work.

References

1. I. BARYCKA and A. MISIUK, *Mater. Sci.* 7 (1981) 465.
2. K. YAJIMA and T. YAMAGUCHI, *J. Mater. Sci.* **19** (1984) 777.

3. Y. CHUNG and H. KIM, *IEEE Trans.* **CHMT-11** (1988) 195.
4. D. N. YOON and W. J. HUPPMAN, *Acta Metall.* **27** (1979) 693.
5. W. A. KAYSEER, S. TAKAJO and G. PETZOW, *ibid.* **32** (1984) 115.
6. W. D. KINGERY, E. NIKI and M. D. NARASIMHAN, *J. Amer. Ceram. Soc.* **44** (1961) 29.
7. W. G. MORRIS, *ibid.* **56** (1973) 360.
8. G. W. GREENWOOD, *Acta Metall.* **4** (1956) 243.
9. I. M. LIFSHITZ and V. V. SLYOZOV, *J. Phys. Chem. Solids* **19** (1961) 35.
10. C. WAGNER, *Z. Elektrochemie* **65** (1961) 581.
11. A. F. SMITH, *Acta Metall.* **15** (1967) 1867.
12. A. J. ARDELL and R. B. NICHOLSON, *J. Phys. Chem. Solids* **27** (1966) 1793.
13. A. J. ARDELL, *Metal. Trans.* **1** (1970) 525.
14. T. K. KANG and D. N. YOON, *ibid.* **9A** (1978) 433.
15. C. H. KANG and D. N. YOON, *ibid.* **12A** (1981) 65.
16. S. S. KANG and D. N. YOON, *ibid.* **13A** (1982) 1405.
17. C. S. JAYANTH and P. NASH, *J. Mater. Sci.* **24** (1989) 3041.
18. R. ASHIMOV, *Acta Metall.* **11** (1963) 72.
19. A. J. ARDELL, *ibid.* **20** (1972) 61.
20. A. D. BRAILSFORD and P. WYNBLATT, *ibid.* **27** (1979) 489.
21. C. K. L. DAVIS, P. NASH and R. N. STEVENS, *ibid.* **28** (1980) 179.
22. P. W. VOORHEES and M. E. GLICKSMAN, *Metal. Trans.* **15A** (1984) 1081.
23. J. A. MARQUSEE and J. ROSS, *J. Chem. Phys.* **80** (1984) 563.
24. M. TOKUYAMA and K. KAWASAKI, *Physica* **123A** (1984) 368.
25. M. TOKUYAMA, K. KAWASAKI and Y. ENOMOTO, *ibid.* **134A** (1986) 323.
26. K. KAWASAKI, Y. ENOMOTO and M. TOKUYAMA, *ibid.* **135A** (1986) 426.
27. R. D. DOHERTY, *Met. Sci.* **16** (1982) 1.
28. A. J. ARDELL, R. B. NICHOLSON and J. D. ESHELBY, *Acta Metall.* **14** (1966) 1295.
29. A. G. KHATURYAN, S. V. SEMONOVSKAYA and J. W. MORRIS Jr, *ibid.* **36** (1988) 1563.
30. W. C. JHONSON, P. W. VOORHEES and D. E. ZUPON, *Met. Trans.* **20A** (1989) 1175.
31. R. D. VENGENOVITCH, *Acta Metall.* **30** (1982) 1079.
32. L. RATKE and K. THIERINGER, *ibid.* **33** (1985) 1793.
33. W. K. THIERINGER and L. RATKE, *ibid.* **35** (1987) 1237.
34. J. M. CHAIX, N. EUSTATHOPWLOS and C. H. ALLIBERT, *ibid.* **34** (1986) 1589.
35. J. M. CHAIX and C. H. ALLIBERT, *ibid.* **34** (1986) 1593.
36. S. C. YANG and P. NASH, *Mater. Sci. Tech.* **4** (1988) 860.
37. E. E. UNDERWOOD, in "Quantitative Stereology" (Addison-Wesley, California, 1970).
38. F. BASHFORTH and J. C. ADAMS, in "An Attempt to Test The Theory of Capillary Action by Comparing The Theoretical And Measured Form of Drop of Fluid" (Cambridge, Cambridge University Press, 1983).
39. R. TERAI and R. HAYAMI, *J. Non-Cryst. Solids* **18** (1975) 217.
40. T. KANEKO, *J. Phys. D* **20** (1987) 489.

Received 30 July 1990
and accepted 12 February 1991